

A multiscale cellular automata model for simulating complex transportation systems

Paweł Topa¹, Witold Dżwiniel¹ and David A. Yuen^{2*}

¹AGH University of Science and Technology, Institute of Computer Science, 30-059 Krakow, Poland

²University of Minnesota, Dept. of Geology and Geophysics, and Minnesota Supercomputing Institute, Minneapolis, MN 55455-0219, USA

Abstract

We present a new two-level numerical model describing the evolution of transportation network. Two separate but mutually interacting sub-systems are investigated: a “starving” environment and the network. We assume that the slow modes of the environment evolution can be modeled with classical cellular automata (CA) approach. We have coarse-grained the fast modes approximating the transportation network by the graph of cellular automata (GCA). This allows the simulation of transportation systems over larger spatio-temporal scales and scrutinizing global interactions between the network and the environment. We show that the model can mimic the realistic evolution of complex river systems. We also demonstrate how the model can simulate a reverse situation. We conclude that the paradigm of this model can be extended further to a general framework, approximating many realistic multiscale transportation systems in diverse fields such as geology, biology and medicine.

Keywords: transportation networks, multiscale systems, graph of cellular automata

Submitted to International Journal of Modern Physics C, February 2006

1 Introduction

Networks are unique structures occurring only in highly self-organized dissipative systems, including biological organisms, geological structures, evolving animal colonies, social and economical systems, computer systems, e.g., [Barabasi, 2002; Turcotte and Rundle, 2002; Newman, 2003]. In biological and environmental sciences, transportation networks play two completely different roles. They help to stimulate growth by disseminating nutrients in the consuming environment or carry away products from productive environment. These two functions are usually carried out simultaneously, as in vascular tissue, road and railway networks and river systems.

The existence of multitudinous topological, biological, morphological degrees of freedom, sharp interfaces between interacting components, multifaceted boundary conditions and self-organized criticality phenomena make the topology of many transportation networks intrinsically very complex. Consequently, due to the difficulty in defining a coherent and integrable functional space, the classical approaches involving partial or ordinary differential equations are extremely difficult to use as a reliable tool, in modeling of these nonlinear systems. Therefore, the existing models prefer statistical methods (e.g., Monte-Carlo simulations [Binder and Heermann, 2002; Merks and Glazier, 2006], diffusion limited aggregation [Masek and Turcotte, 1993; Turcotte and Newman, 1996; Baish and Jain, 2000], statistical mechanics [Turcotte, 1999]), percolation [Sahimi, 1994; Stark, 1991] and cellular automata (CA) [Wolfram,

2002; Murray and Paola, 1994]), which employs a set of scientific rules instead of nonlinear partial differential equations. However, all of these approaches ignore multi-scale interactions between the network and evolving environment. Therefore, although successful in simulating homogeneous systems, they cannot be used for modeling systems involving complex multiresolutional topology, such as anastomosing systems.

The term *anastomosis* comes from the medical sciences and is defined both as a surgical connection between 2 structures or the network of connecting channels e.g., between veins of leaves, rivers, etc. Anastomosing networks of river channels and blood vessels are usually formed by natural disturbances in flow channels, e.g. caused by processes of angiogenesis or erosion/blocking in river channels, which produce bifurcations, loops and avulsions. These structures cannot come from relatively fast processes of sediment transportation and accumulation in rivers [Makaske 2001] or formation of anastomoses due to atherosclerosis in blood vessels (e.g., [Mils and Everson, 1991]). They are stimulated mainly by the slow modes of environmental growth factors (e.g., the vascular system in [Gamba et. al., 2003]).

In this paper we consider the hypothesis of “starving environment” [Topa and Paszkowski, 2002] as a focal point of transportation systems expansion. For example, in the anastomosing river system, the peat-bog can be regarded as the “starving environment”. It means that the supply of nutrients is insufficient, they are consumed very fast and the peat-bog growth is restrained. Analogously, “starving” tumor cells in hypoxia, in response to the lack of oxygen produce VEGF (*vascular endothelial growth factor*). This factor stimulates the fast growth of vascular tissue in the complex process of angiogenesis [Mazure et al., 1996]. Conversely, “starving” plant explores a productive environment by the huge network of roots in search for water and minerals [Persson, 1990]. The roads and railway systems grow towards emerging industrial economic centers (e.g., [Yerra and Levinson, 2005]). These factors accelerate the expansion of the transportation network towards “hungry” areas. The positive feedback interaction between two factors: the network and environment, results in a mutually supported growth. On the other hand, dysfunction in mechanisms stimulating the network expansion results in the death of the entire system.

The dynamics of these complex networks involves multiple spatio-temporal scales. The local interactions between the fast modes corresponding to transport (flow) and slow time scales represented by the environmental factors, make the models based on classical CA paradigm too computationally stiff. In this paper we propose a novel approach. We employ the graph of cellular automata data structure, which allows for coarse-graining of the fast flow modes and cover larger spatio-temporal scales than former fine grained CA model [Topa and Paszkowski, 2002]. As an example of the complex transportation network, we simulate anastomosing river system. We also demonstrate that this approach can be generalized to other problems, which promulgate the “starving environment” paradigm.

The paper follows this plan. First, we discuss both advantages and limitations of the fine grained CA model for modeling of anastomosing river system. Then, we define a new model in which the graph of cellular automata was used for coarse graining of the fastest flow modes in the fine grained CA system. Finally, we present the results of modeling and in the conclusions we discuss generalization of the model especially towards modeling other types of transportation systems.

2 Fine-grained model of river systems

Fine-grained model of river system can employ the cellular automata paradigm (e.g. [Chopard and Droz, 1998]) in a classical manner (see e.g., [Rodriguez-Iturbe and Rinaldo, 1997; Topa and Paszkowski, 2002]). The terrain can be represented by a rectangular mesh of computational cells. The state of each cell describes parameters corresponding to altitude, water amount, nutrient densities and peat layer thickness. Automata evolve according to the rules, which govern water

flow, nutrient distribution, peat accommodation and bottom-channel sedimentation. In the cellular automata model [Topa and Paszkowski, 2002] both the Moore neighborhood and the fixed boundary conditions were used. The borders of the mesh were simulated as extremely high barriers, which prevent horizontal dissipation of water from the simulation domain. A portion of a real anastomosing system is shown in Fig.1.

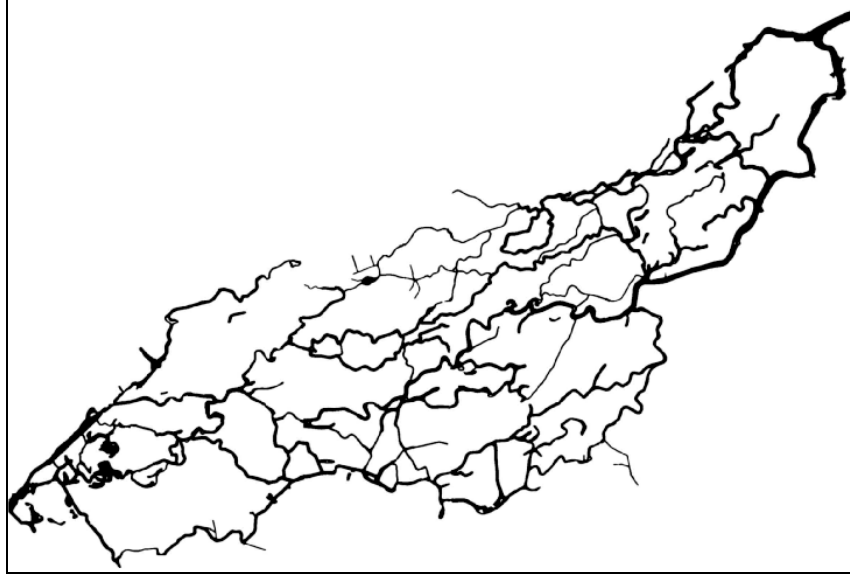


Fig.1 A portion of a realistic anastomosing system in Poland (illustration courtesy of Professor Gradziński [Gradziński et.al. 2000]). The part of the river shown here is about 8 km long and up to 2 km wide.

The model consists of four procedures employed at each timestep (see Appendix, Algorithm1 and 2). The procedures **supply_water()** and **remove_water()** add water to the inlet and remove water from the outlet, respectively. Distribution of the water from cell to its closest neighbors is achieved by the procedures **calculate_flow()** and **update_water()**. The rule is homogeneous for the whole CA system. It mimics the process of water distribution due to gravitation, using the procedure of minimizing the differences in the water levels in the neighboring cells [Topa, 2000; 2005]. The procedure **distribute_nutrients()** calculates the concentration of nutrients in the neighborhood of cells with non-zero water layer. The nutrients concentration influences the thickness of the peat bog layer in “dry” cells (**update_peatbog ()** procedure). The growth is proportional to the current concentration of nutrients with a proportionality coefficient. Moreover, in each cell containing water the process of sedimentation occurs. Therefore, the height of terrain in these cells increases (see procedure **update_terrain ()** in the Appendix, Algorithm 2). We assume that at each timestep it grows proportionally to the current amount of water in the cell.

In Fig.2 we illustrate the snapshots from simulations for a cellular automata 530x530 mesh. The river runs in a valley with very steep barriers in the borders parallel to the mainstream. The terrain is slightly inclined (the slope is 0.05%) and rough. However, the vertical random amplitude of roughness is assumed to be small and less than 1% of the distance between neighboring cells. Water is supplied to the system by a single source cell. We show snapshot from simulation after 5×10^4 timesteps in Fig.2 and compare this to a small fragment of the river from Fig.1. We can observe the creation of small floods in the two pictures and similar backbone structure. The result from Fig.2a shows the fine grained structure not discernible in the scale of Fig.1 due to smoothing.

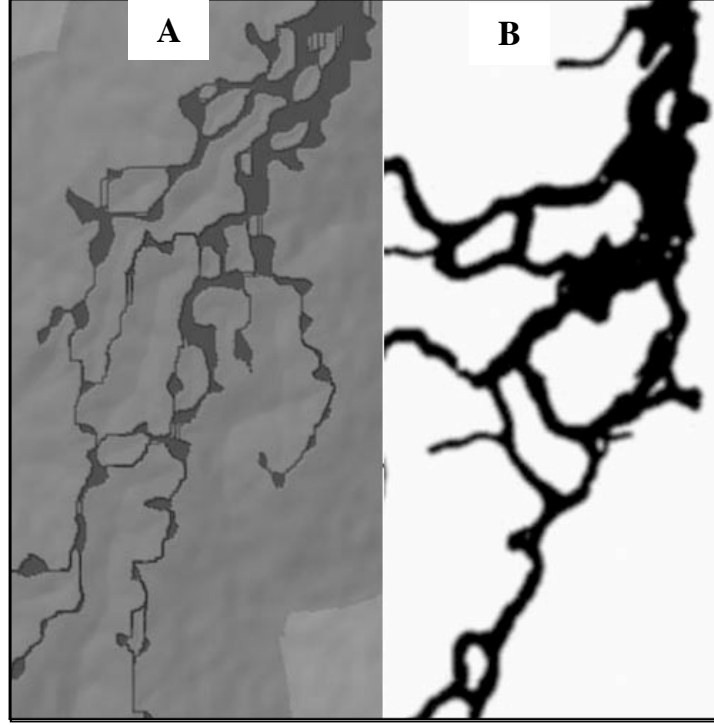


Fig.2 Comparison of modeled river channels (A) to a small fragment of the river from Fig.1 (B).

The main disadvantage of classical CA model is its slow computational speed for simulating more and more disparate spatio-temporal scales. This is mainly due to high degree of spatial and temporal disparity between the processes modeling the evolution of anastomosing system. The flow velocity of the river is orders of magnitude greater than environmental changes, such as the peat-bog growth and sedimentation. This assumes that the configuration of the terrain does not change too much. The channels are too shallow, resulting in wide floods. Modeling realistic anastomosing networks with our CA model would involve with at least 10^6 - 10^8 cells and a similar number of time steps.

3 Graph of cellular automata in modeling of anastomosing networks

We propose a novel approach, which postulates the local degrees of freedom, smaller than the macroscopic, could be eliminated by their coarse grained representation. This can be achieved by a partial separation of the two time scales represented by formation of the channel and the environmental factor (peat-bog growth), respectively. Instead of modeling local in-cell relations between the amount of water (and nutrients) and peat-bog height, we consider now the global interactions between the entire network and environment. The network edges (river channels) can be added or removed according to the current terrain configuration. Conversely, the terrain configuration is formed by the entire river network. The feedback between environmental changes and evolution of the network should be faster allowing for modeling anastomosing systems over larger spatial scales.

Similar to our CA model, we represent the anastomosing system by a mesh consisting of cellular automata. We model the distribution of nutrients and environment growth in the same way as before, while the model of water distribution is completely different. As shown in Fig.3, we define the transportation network as a graph of cellular automata (GCA) located on top of the CA mesh. We note here that the river channels represent the edges, while the junctions and

bifurcation points denote the graph nodes [Topa and Paszkowski, 2002; Topa and Dzwinel, 2004].

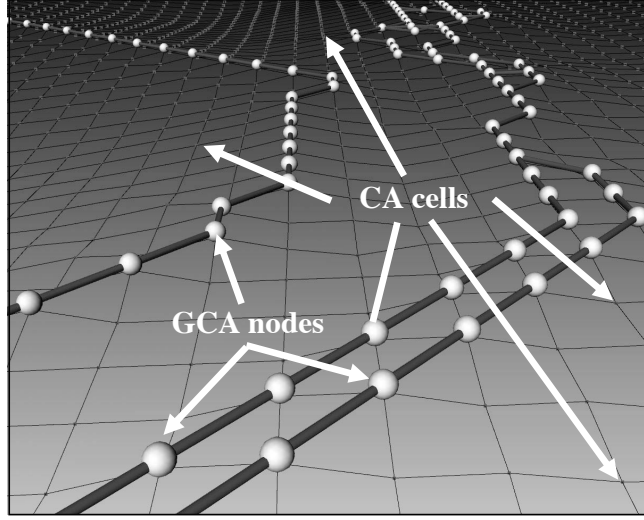


Fig.3 The transportation network is represented by a graph of cellular automata (GCA), while the environment is modeled by the CA mesh. The GCA nodes overlap the CA cells.

The inbank capacity r and flow velocity f in a fragment of river channel are the additional components of the state vector $[g, n, p]$, describing the height of the terrain g , nutrients concentration n and thickness of the peat-bog layer p , respectively. The inbank capacity and the flow velocity are defined only for the cells corresponding to GCA nodes. These cells represent also the nutrient sources.

Algorithm 3 from the Appendix illustrates the general idea of the new coarse-grained model. The entire system is asynchronous due to both different time scales and the evolution rules applied to the two principal components of the model, i.e., the transportation network (GCA) and the environment (CA). All the cells from GCA are updated in the order resulting from the depth-first-search algorithm. The procedures from Algorithm 2 (see the Appendix): **update_throughput ()** and **update_flows()** start the update from source cells. The other CA cells are updated synchronously, assuming that the network update is just finished. Thus the two time scales responsible for the environment and river channels growth are split up, respectively.

Our system can be defined in a formal way as follows:

$$CA_{GR} = \langle Z^2, X_K, G_{CA}, A_I, X_G, S, \delta_K, \delta_G \rangle \quad (1)$$

where:

Z^2 – size of the system representing $Z \times Z$ square mesh of cellular automata,

G_{CA} – a planar and acyclic graph defined as (V_G, E_G) , where $V_G \in Z^2$ and $E_G \in Z^2 \times Z^2$ are a finite set of vertices and a finite set of edges, respectively,

A_I – a set of sources, $A_I \in V_G$,

X_{Kij} – the set of neighboring cells for (i, j) cell, which does not belong to the G_{CA} graph,

X_{Gij} – the set of neighboring cells for (i, j) cell, which does belong to the G_{CA} graph and

$$X_{Gij} = (i, j) \cup \{(k, l) : (k, l) \in V_G, [(i, j), (k, l)] \in E_G\},$$

S – is the set of state vectors corresponding to each cell.

We define two types of the state vector. The first one defined for all the CA cells and the second one only for the GCA graph nodes. They are as follows:

1. The state vector of the cells from the environment (g,n,p) , where:
 - a. g – height of the terrain,
 - b. n – nutrient concentration,
 - c. p – thickness of the peat-bog layer.
2. The state vector in the nodes of GCA transportation network (f,r) where:
 - a. f – flow velocity,
 - b. r – the inbank capacity of a fragment of the river channel.

Two transition functions $\delta_K()$ and $\delta_G()$ are defined by:

$$(g_{ij}^{t+1}, n_{ij}^{t+1}, p_{ij}^{t+1}) = \delta_K((g_{ij}^t, n_{ij}^t, p_{ij}^t)) \quad (2)$$

$$(f_{ij}^{t+1}, r_{ij}^{t+1}) = \delta_G((f_{ij}^t, r_{ij}^t)) \quad (3)$$

and represent the two sets of rules. The first set (2) is applied in a synchronous way for each CA cell, while Eq.(3) defines the changes in every cell belonging to V_G nodes.

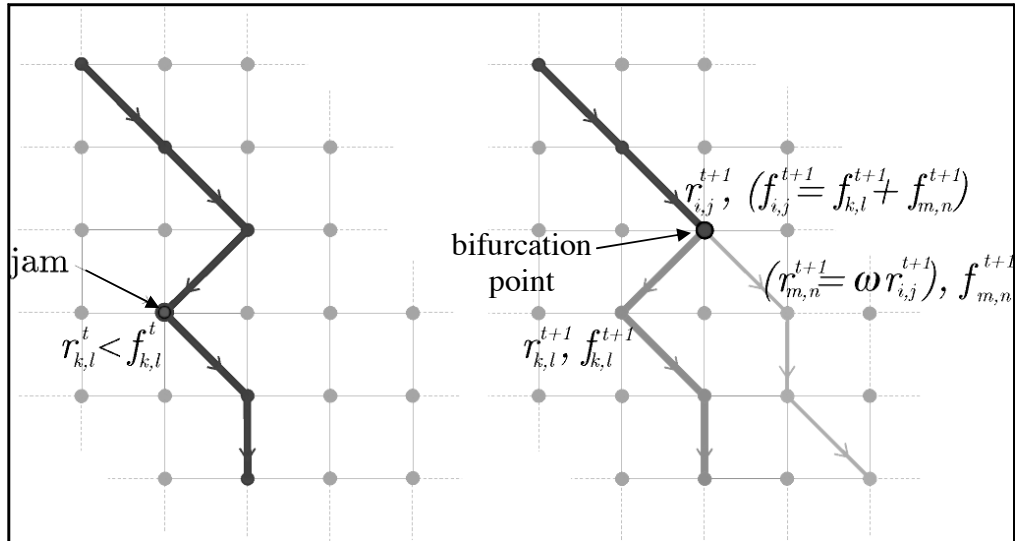


Fig.4 The process of formation of a new network channel due to the jam in (k,l) G_{CA} graph node. The new channel is formed in preceding (i,j) node and its inbank capacity is equal to ωr_{ij} , where $\omega < 1$ and r_{ij} is the inbank capacity of the parent channel, respectively. The flow intensity f_{ij} in the parent channel is the sum of flows in the descending channels.

The values of f in GCA nodes are updated sequentially in order, which corresponds to water propagation from the source cells A_1 to all graph nodes $(i,j) \in V_G$. At the bifurcation points the value of flow intensity f is shared between two channels proportionally to the inbank capacity value r . On the other hand, at the junction points the values of f of converging channels are added. A slow decrease of the inbank capacity (e.g., due to excessive growth of plants and sedimentation) is modeled by a linear decrease of r_{ij} .

However, in realistic situations, the inbank capacity r can be jammed radically by larger obstacles (fallen trees, floes etc.). A certain decrease in r can amplify greatly. The material carried by the river current can be stopped by the obstacle, which usually results in fast obstruction. We model this behavior by defining a given threshold r_0 below which the current

inbank capacity r decreases as fast as $1/r$. As illustrated in Fig.4, in the case of complete blockage, i.e., $f_{ij} > r_{ij}$, a new channel is formed just above the node of obstruction.

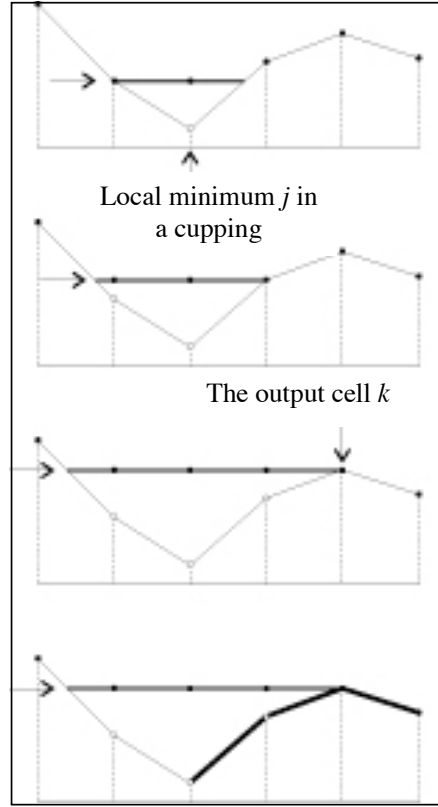


Fig.5 The iterative procedure for searching the outlet from a local flood. The neighboring cells of the “lowest” cell j - sorted in order of increasing terrain height - are searched bottom-up and labeled. The first encountered cell k , which has an unlabeled neighbor situated “lower” than k , is the outlet from the cupping. The “escape path” from the local minimum is displayed in bold line.

We assume that:

1. The initial inbank capacity of the new channel r_{mn} is smaller than the in the parent channel r_{ij} and $\omega = r_{mn}/r_{ij} < 1$,
2. the average value of ω (see Fig.5), estimated empirically, is about 0.25,
3. the direction of the r_{mn} channel is computed locally by the steepest descent method.

Initially, the **update_flows** () procedure (see Algorithm 3 in the Appendix) searches the nearest neighbors of the bifurcation node (i,j) (or in the following steps - the cell recently added to the GCA graph) looking for the cell (k,l) , which is situated below the node, i.e., $H_{kl} < H_{ij}$ (where $H_{ij} = g_{ij} + p_{ij}$ is local elevation in the cell (i,j)). If this does not exist, we execute a procedure **find_way_from_cupping**() - illustrated in Fig.5. The time loop is repeated, until a newly forming channel meets another channel or reaches the boundary of the CA mesh.

4 Modeling results

As an outcome of modeling of the anastomosing system, we obtain:

1. the graph structure representing the overall river network,
2. the CA mesh, which mimics the terrain configuration.

Due to coarse graining of the CA model by the graph of automata approximation, we obtain a much clearer global view of anastomosing system in “starving environment”. As displayed in Fig.6 and Fig.7, we can visualize the channels as pipes, whose diameter represents the inbank capacity, while the color reveals the intensity of the flow. Flow intensity defines how much water is transported in the unit of time through the channel (defined from node to node). We can also visualize the hierarchical structure of the channels (Fig.6). This information can be very helpful in comparative studies. Our model does not consider other geological factors, e.g., differentiation of peat-bog density by gravitational setting. In realistic situations this peat-bog density differentiation will produce a smoother terrain configuration.

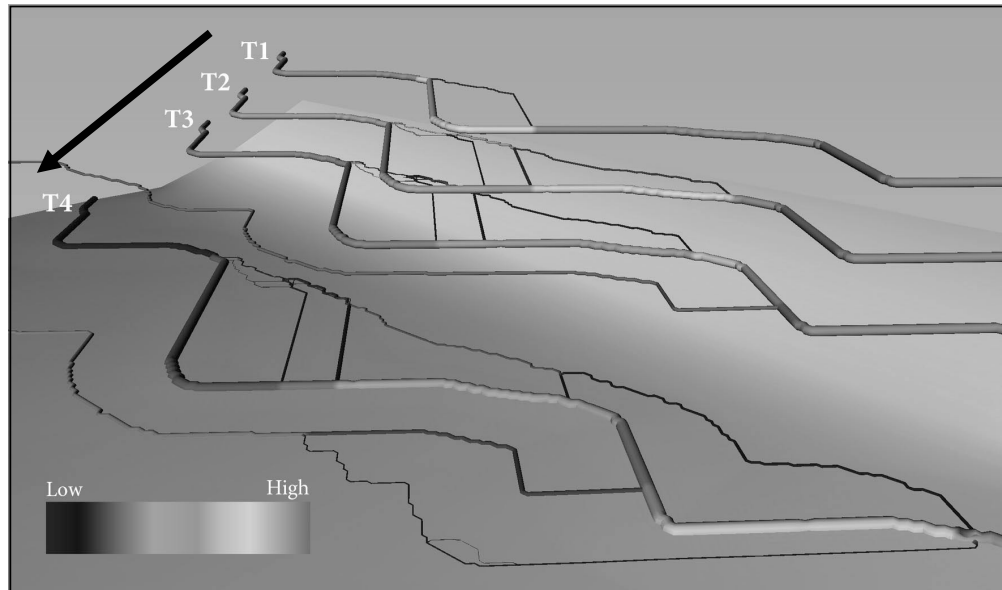


Fig.6 The GCAs display evolution of the river network in successive timesteps T1, T2, T3, T4. The diameter of the pipe represents the inbank capacity, while their color shows the flow intensity in the channels (the highest is red). The 3-D Amira visualization package (www.amiravis.com) was employed.

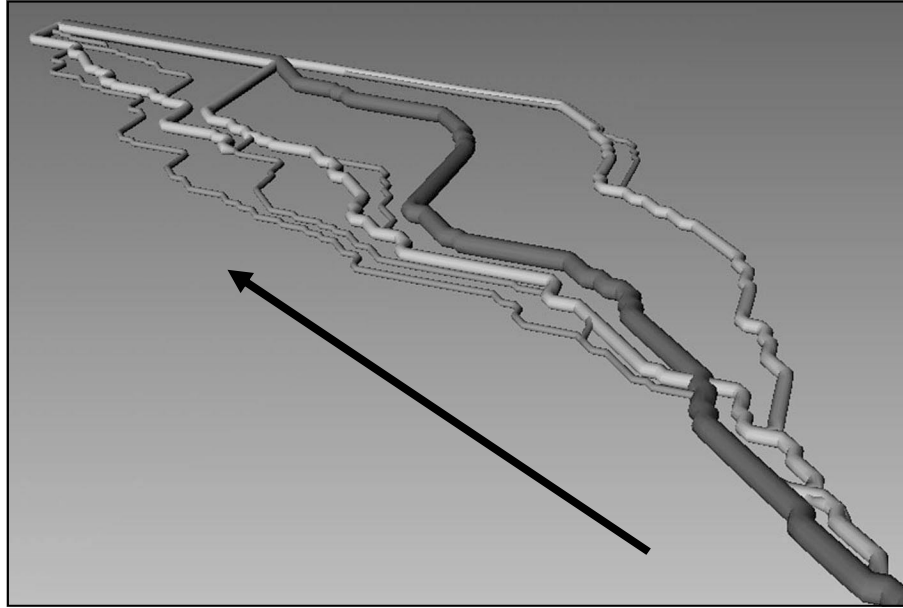


Fig.7 The branch-join river channels generated by GCA model. The channels of various flow intensity and inbank capacity can be easily recognized. The Amira visualization package was employed.

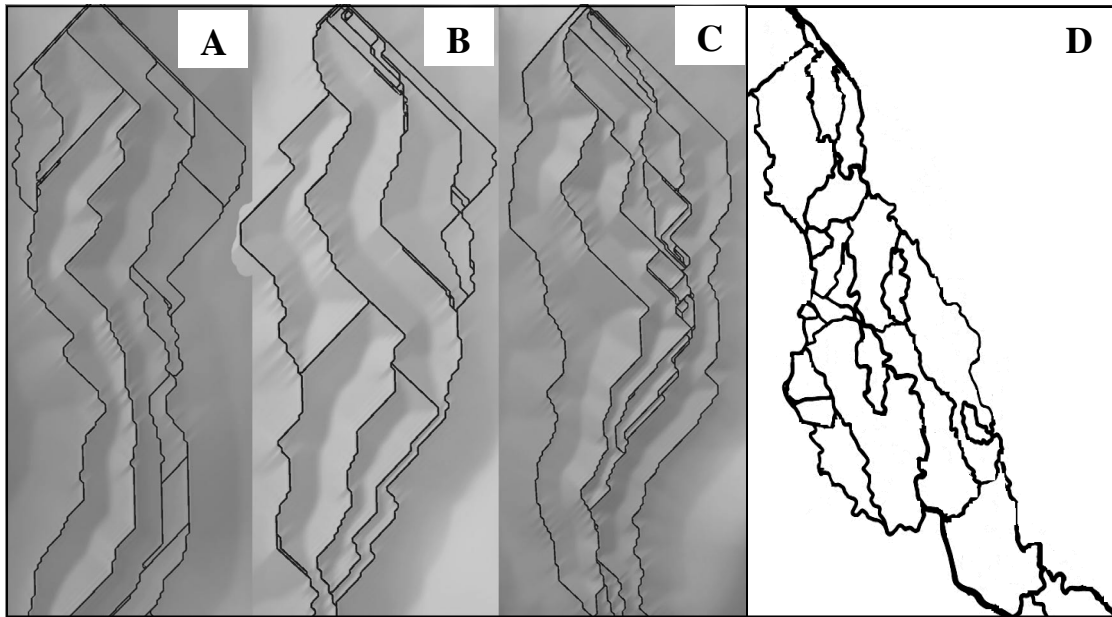


Fig.8 The typical snapshots from simulation of anastomosing system obtained for GCA model after 1500 time-steps (corresponding a few years in observations). The initial random configurations of the terrain (A,B,C) were slightly different for each of these three cases (mesh size is 329×329 points, initial terrain inclination was 0.02%). The results are compared to the realistic anastomosing river system (D).

In Fig.8 we display a few snapshots from simulations of anastomosing channels for different initial conditions. Unlike the situation shown in Fig.2, which focuses on a small fragment of the

river, the GCA produces a global view of anastomosing system. There we can clearly recognize the network of branch-joining channels and loops, which mimics well the backbone of the real river structure. To be sure, the anastomosing system from Fig.1 reveals far more details than the results of our simulation. They can be partly improved by using larger CA systems simulated over a longer time. Further advances can be made by considering processes neglected in this model, (e.g., erosion) and by employing a more accurate model for sedimentation.

However, some microscopic structures, such as dead end channels and flooded areas, clearly shown in Fig.1, cannot be simulated. This drawback is mainly due to the coarse graining of the local flow-environment interactions. Instead, as shown in Fig.3, these microstructures can be produced by the fine grained CA model.

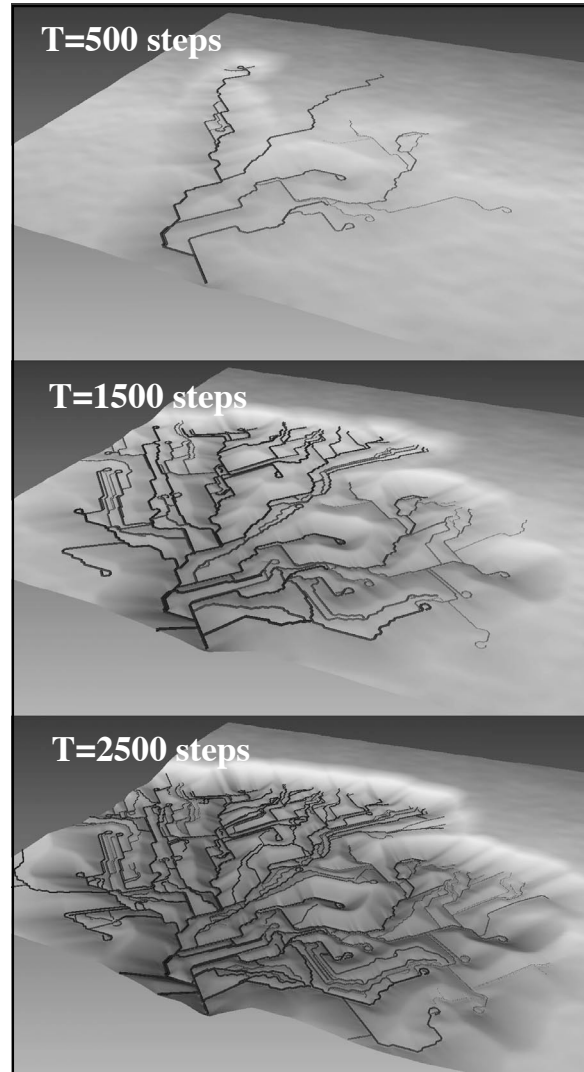


Fig.9 Snapshots with time from GCA simulation of the transportation network in a productive environment.

Unlike in anastomosing systems, the network in productive environment moves away its resources. We show this in Figs.9,10 by the changes in the “landscape” of resources concentration. The system converges to the state in which the entire environment area will be

uniformly drained. The characteristic loops observed at the tips of some channels in Figs.9,10 correspond to the local maxima of the nutrient concentration.

Our results of modeling appear very similar to the dendritic networks [Wittmann, et. al., 1991]. This type of systems is a very good example of fractal trees occurring as a universal pattern in nature [Mandelbrot, 1982; La Barbera and Rosso, 1987; Newman et al., 1997; Turcotte 1997]. The nutrients concentration field looks like terrain configuration shaped by erosion. Nevertheless, this model cannot describe the dynamics of eroding river networks in an exhaustive way. First, the networks in a productive environment consist of roots and leaves, while realistic river systems are produced due to merging of channels. Second, we use the algorithm of the steepest descent, which allows for unrealistic behavior in case of rivers simulation. For example, the edge of simulated network can go along the hogback, while a realistic river channel will be directed downstream.

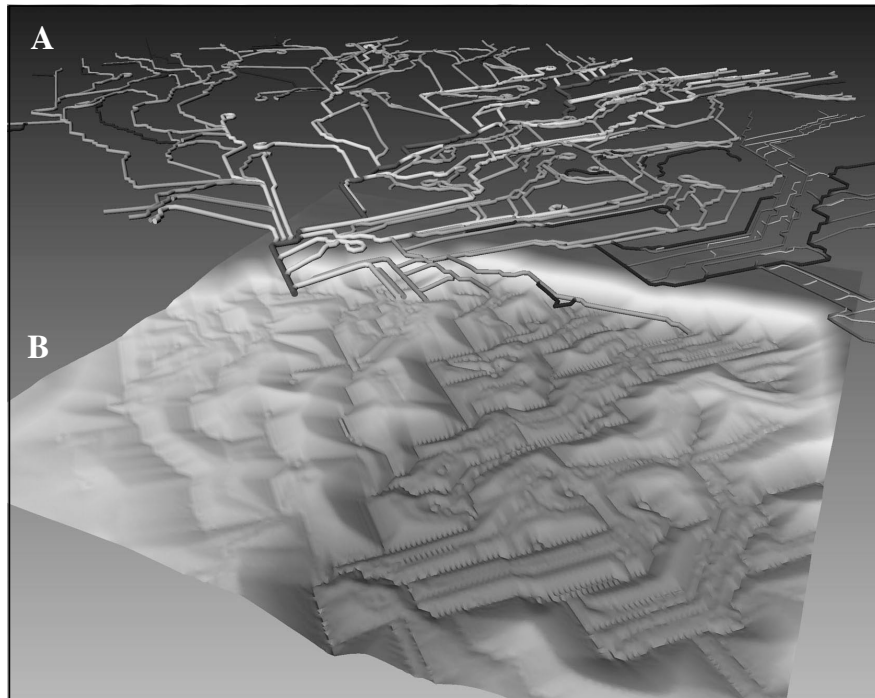


Fig.10 Branching transportation network (A) from Fig.9 with hierarchy of channels and the “landscape” of nutrients concentration (B) created by this network (red color denotes the highest concentration of nutrients).

5 Concluding Remarks

Visual inspection is insufficient for comparing results from a computational model to real systems. Statistical verification of our model could be possible by employing network descriptors, such as these defined in [Dodds and Rothman, 1999; 2001a,b,c; Rodriguez-Iturbe and Rinaldo, 1997; Pelletier and Turcotte, 2000]. However, the structures of the real transportation networks change dynamically in a chaotic way and depend on a huge amount of geological, biological and sociological factors. Small fluctuations may cause dramatic changes in the final pattern produced by the system. Therefore, to pass statistical verification, our model should be supplemented by complex paradigms involving geological processes including erosion, sedimentation [Makaske, 1998] and geomorphologic models [Murray and Paola, 1996;1997]. These multi-scale processes

can be described in terms of partial differential equations [Makaske, 1998] and discrete particle models [Dzwinel and Yuen; 2000a;b].

We realize that our two-level cellular automata model can only serve initially as a general framework, when applied to realistic systems. We have shown that coarse graining of cellular automata model allows for a substantial reduction of the number of microscopic degrees of freedom. Thus the model can be expanded over larger spatio-temporal scales. Moreover, the results of simulation of anastomosing system confirm the “starving environment” hypothesis [Topa and Paszkowski, 2002] in which the transportation network is driven by a consuming (starving) environment. In the case of anastomosing rivers, the terrain configuration, changed dynamically by the peat-bog growth, stimulates the proper spreading of nutrients and expansion of the transportation network structure towards the “starving” areas. However, we should emphasize that the convergence of CA model to GCA is only a plausible hypothesis and should be verified more formally.

Due to the coarse graining, small floods and dead channels, resulting from the local interaction between the main flow and terrain, cannot be modeled. The width of all the channels simulated by the graph of cellular automata is the same and independent on the flow intensity and channel inbank capacity. This disturbs additionally the local structure of the system and does not allow for including erosion to the system in a self-consistent manner. To overcome these defects, a new multiscale model is sorely needed. This can be constructed on the basis of the two presented approaches: the fine grained CA and the coarse grained GCA models. Once the new channels are created in the coarse grained system, the area of channels creation are zoomed in and tuned by the CA paradigm. The modifications can, in turn, be fed back to the coarse grained model.

As shown by [Pelletier and Turcotte, 2000], driving forces producing transportation networks can be scaled independently and can act in a similar way, regardless of their origin, e.g. the capillary system in leaves is very similar to some river systems. Therefore, understanding the explicit mechanisms for creating transportation networks can be very useful and be expanded to search similarly acting agents in many important biological networks such as vascular system [Gamba et. al., 2003; Merks and Glazier, 2006].

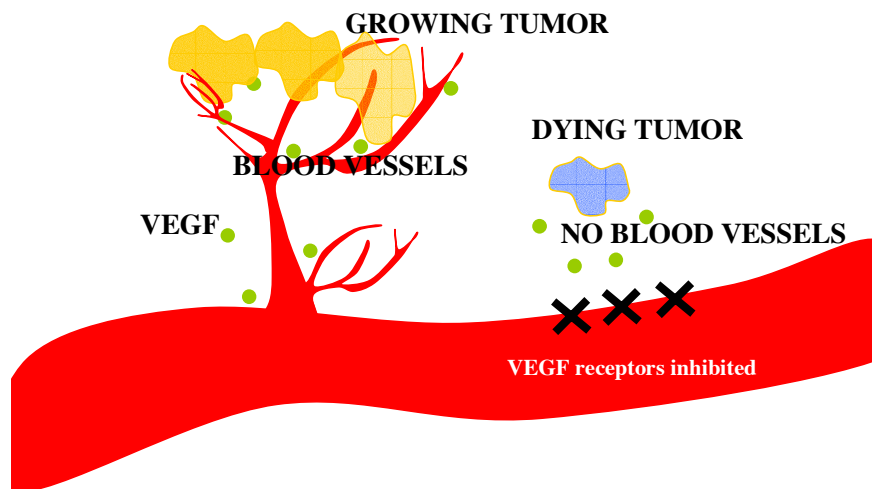


Fig.11 Conceptual picture of vascular network created in the process of angiogenesis.

Modeling of the transportation networks in biology is crucial not only in understanding the complexity of organisms but also for recognizing the factors, which control their growth. For example, as shown in Fig.11, by inhibiting receptors of VEGF – the factor which is responsible

for development of the vascular system in the process of angiogenesis (e.g. [Yancopoulos et al., 2000; Coultas et al., 2005; Folkman, 2006]) – the growth of vascular tissue can be stopped. Consequently, tumor cells will die from “starvation”. The multi-scale models of angiogenesis based on the graph of cellular automata could give us a very unique opportunity to scrutinize the family of microscopic factors influencing this amazing global behavior.

Acknowledgments

This research is partly financed by the Polish Committee of Scientific Research KBN, Grant No. 3T11C05926 and Math-Geo Program of N.S.F.. W.D. thanks Institute of Mathematics and its Application (I.M.A.) at the University of Minnesota for support. The authors are grateful to Dr Mariusz Paszkowski, Professor Dr R. Gradziński and Professor Dr Bob Criss for their contributions to this paper.

References

- Baish J., W., Jain R., K., Fractals and Cancer, *Cancer Research*, 60:3683-3688
- Barabasi A-L. (2002). *Linked:The New Science of Networks*. Perseus Books Group, Cambridge, MA, pp. 265.
- Binder, K and Heermann, D.W., (2002). *Monte Carlo Simulation in Statistical Physics: An Introduction* (Springer Series in Solid-state Sciences S.) Springer-Verlag Berlin and Heidelberg GmbH & Co. K, pp. 192.
- CODGiK (1985). Mapa topograficzna w skali 1:25 000. Wydane przez Centralny Ośrodek Dokumentacji Geodezyjnej i Kartograficznej, *Center of Cartography Documentation – Poland*, <http://www.codgik.waw.pl/>.
- Chopard, B., and Droz, M., (1998). *Cellular Automata Modeling of Physical Systems*. Cambridge University Press.
- Coultas L., Chawengsaksophak K., Rossant J., (2005). Endothelial cells and VEGF in vascular development, *Nature*, 438: 937-946.
- Dodds, P.S., and Rothman, D.,H., (1999). Unified view of scaling laws for river networks. *Phys. Rev. E*. 59 (5): 4865-4877.
- Dzwinel W, Yuen D.A, (2000a). A two-level, discrete particle approach for large-scale simulation of colloidal aggregates, *Int. J. Mod Phys.C*, 11/5:1037-1067.
- Dzwinel W, Yuen D.A, (2000b). A Multi-level Discrete Particle Model in Simulating Ordered Colloidal Structures, *J Colloid Int Sci*, 225:179-190.
- Folkman J., (2006) Angiogenesis. *Annual Review of Medicine*, 57:1-18.
- Gamba, A., Ambrosi, D., Coniglio, A., de Candia, A., Di Talia S., Giraudo, E., Serini, G., Preziosi, L., Bussolino, F., (2003). Percolation, Morphogenesis, and Burgers Dynamics in Blood Vessels Formation, *Phys. Rev. Lett.*, 90(11): 118101-4.

Gradziński, R., Baryła, J., Danowski, J., Doktor, M., Gmur, D., Gradziński M., Kędzior A., Paszkowski, M., Soja, R., Zieliński, T., Żurek, S., (2000). Anastomosing System of Upper Narew River, NE Poland, *Annales Societatis Geologorum Poloniae*, 70:219-229.

Kramer, S., and Marder M., (1992). Evolution of river networks. *Phys. Rev. Lett.* 68:205-209.

La Barbera, P. and Rosso, R., (1987). The fractal geometry of river networks, *EOS Trans. AGU*, 68, 1276.

Makaske, B. (1998). Anastomosing rivers: forms, processes and sediments. Netherlands Geographical Studies 249. Utrecht: Royal Dutch Geographical Society. 298 pp., ISBN: 90 6809 271 5.

Makaske, B., (2001). Anastomosing rivers: a review of their classification, origin and sedimentary products, *Earth-Science Reviews*, 53(3/4):149-196.

Makaske B., Smith. D., G., Berendsen, HJ.A., (2002). Avulsions, channel evolution and floodplain sedimentation rates of the anastomosing upper Columbia River, British Columbia, Canada. *Sedimentology*. 49:1049-1071

Mandelbrot, B., (1982). *The Fractal Geometry of Nature*, Freeman Co., San Francisco.

Mazure, N, Chen, E., Laderoute, K, Giaccia, A, (1996). Oncogenic transformation and hypoxia synergistically act to modulate vascular endothelial growth factor expression. *Cancer Research*, 56(15), 3436-3440.

Masek, J.G. and Turcotte, D.L. (1993). A diffusion-limited aggregation model for the evolution of drainage networks, *Earth and Planetary Science Letters*, 119:379-386.

Medical Encyclopedia, <http://www.nlm.nih.gov/medlineplus/ency/article/002231.htm>.

Merks R.M.H., Glazier J., A., (2006). Dynamic mechanisms of blood vessel growth. *Nonlinearity* 19(1):C1-C10.

Mills N., L., Everson C., T., (1991). Atherosclerosis of the ascending aorta and coronary artery bypass. Pathology, clinical correlates, and operative management, *The Journal of Thoracic and Cardiovascular Surgery*, 102: 546-553

Murray, A.B., and Paola, C., (1994), A cellular model of braided streams: *Nature*. 371: 54-57.

Murray, A.B., and Paola, C., (1996), A new quantitative test of geomorphic models, applied to a model of braided streams: *Water Resources Research*. 32: 2579-2587.

Murray, A.B., and Paola, C., (1997), Properties of a cellular braided-stream model: *Earth Surface Processes and Landforms*. 22:1001-1025.

Newman, M.E.J., (2003). The structure and function of complex networks. *SIAM Review*, 45(2): 167-256.

Newman, W.I., Turcotte, D.,L., Gabrielov, A., M., (1997), Fractal trees with side branching. *Fractals*, 5/4:603-614.

Pelletier J.D., and Turcotte, D.L., (2000). Shapes of river networks and leaves: are they statistically similar. *Phil.Trans.R.Soc.Lond.* 355:307-311.

Persson, H., (1990). Methods of studying root dynamics in relation to nutrient cycling. In *Nutrient Cycling in Terrestrial Ecosystems. Field Methods, Application and Interpretation*. Eds. A F., Harrison, P., Ineson and O., W., Heal. 198–217. Elsevier Applied Science, London.

Rodriguez-Iturbe I., and Rinaldo, A., (1997). Fractal River Basins. Chance and Self-Organization. Cambridge University Press.

Sahimi, M., Applications of Percolation Theory, (1994). Taylor and Francis 258 pp.

Stark, C.P., (1991). An invasion percolation model of drainage network evolution. *Nature* 352:423-427.

Topa, P., (2000). River flows modelled by cellular automata. In M. Bubak, J. Mościński, and M. Noga (eds.), Proceedings of The First Worldwide SGI Users Conference, Kraków, Poland. Academic Computer Centre, CYFRONET. ISBN 83-902363-9-7.

Topa, P., and Paszkowski, M., (2002). Anastomosing transportation networks. In Wyrzykowski R. et al. (ed.), Proc. Of 4th International Conference, Parallel Processing and Applied Mathematics PPAM '01, vol. 2328 of *Lecture Notes in Computer Sciences LNCS*, pp. 904-911. Springer-Verlag, Berlin, Heidelberg.

Topa, P., and Dzwinel, W., (2004). Consuming environment with transportation network modelled using graph of cellular automata. In R. Wyrzykowski et al. (ed.), Parallel Processing and Applied Mathematics, PPAM 2003, vol. 3019 of *Lecture Notes in Computer Science LNCS*, pp. 513-520. Springer-Verlag.

Topa P., (2005). Computational Models of Growth Phenomena in Geology, Ph.D thesis, AGH University of Science and Technology, Krakow, Poland, pp 157 (in Polish)

Turcotte, D.,L. (1997), Fractals and Chaos in Geology and Geophysics, 2nd Edition, University of Cambridge, U.K., 398 pages

Turcotte, D.,L., (1999), Applications of statistical mechanics to natural hazards and landforms, *Physica A*, 274:294-299.

Turcotte, D.L, and Newman, W.I. (1996). Symmetries in geology and geophysics *Proc. Natl. Acad. Sci. USA.* 93:14295-14300

Turcotte, D.L., and Rundle, J.B., (2002). Self-organized complexity in the physical, biological and social sciences, *Proc. of the National Academy of Sciences.* 99:2463-2465.

Wolfram S (2002) *A New Kind of Science*, Wolfram Media Incorporated. pp. 1263

Yancopoulos GD, Davis S, Gale NW, Rudge JS, Wiegand SJ, Holash J. (2000). Vascular-specific growth factors and blood vessel formation. *Nature* 407:242-248.

Yerra, B., M., and Levinson, D., M., (2005). The emergence of hierarchy in transportation networks, *The Annals of Regional Science*, 39(3): 541-553.

APPENDIX

1. Fine-grained cellular automata model – procedures and algorithms

Let us define this cellular automata (CA) model as follows:

$$CA_{\text{FLOW}} = \langle Z^2, A_s, X, S, \delta \rangle \quad (\text{A1})$$

where:

Z^2 – is the size of the system representing the $Z \times Z$ square mesh of cellular automata,

$A_{in} \in Z^2$ – set of cells modeling sources - inlets,

$A_{out} \in Z^2$ – set of cells modeling outlets,

X_{ij} – the set of neighboring cells for (i,j) cell,

(i,j) – is the location of the cell on the mesh,

$S = \{(g_{ij}, w_{ij}), i, j = 1, \dots, Z\}$ – the set of vector states describing (i,j) cell,

g_{ij} – the height of the terrain in (i,j) cell,

w_{ij} – the thickness of water layer in (i,j) cell.

δ - is a transition function defined as follows: $(g_{ij}, w_{ij}^{t+1}) = \delta((g_{ij}, w_{ij}^t))$.

The water level s_{ij}^t in cell (i,j) and time t is defined as follows:

$$s_{ij}^t = g_{ij} + w_{ij}^t. \quad (\text{A2})$$

The cellular automata for anastomosing river can be defined as in Eqs.(1), assuming that:

$S = \{(g_{ij}, w_{ij}, n_{ij}, p_{ij}), i, j = 1, \dots, Z\}$ – the set of vector states describing (i,j) cell,

g_{ij} – the height of the terrain in (i,j) cell,

w_{ij} – the height of water in (i,j) cell,

n_{ij} – concentration of nutrients,

p_{ij} – the peat-bog thickness.

δ - is a transition function defined as follows: $(g_{ij}^{t+1}, w_{ij}^{t+1}, n_{ij}^{t+1}, p_{ij}^{t+1}) = \delta((g_{ij}^t, w_{ij}^t, n_{ij}^t, p_{ij}^t))$.

The height of terrain g_{ij} in the cells increases. We assume that it grows at each timestep proportionally to the current amount of water in the cell (i,j) , i.e., as

$$g_{ij}^{t+1} = g_{ij}^t + w_{ij}^t. \quad (\text{A3})$$

Below we present the algorithms:

Algorithm 1 The CA model of water spreading in the terrain

repeat

supply_water (); {add water to the inlets}

remove_water (); {remove water from the outlets}

calculate_flow (); {calculate amount of water distributed between the cells}

update_water (); {update water in cells}

until $the_number_of_timestep > T$

procedure calculate_flow();

reset_flow_table ($f=0$);

{initialize the water redistribution array}

for each *cell* (i,j) do begin

$E := \{(i,j)\}$;

{the set of cells eliminated from calculations}

repeat

$$s_{avg}^{ij} = \frac{\sum_{(k,l) \in X(i,j)-E} s_{kl}^t}{n}; \text{ {calculate average water level in the neighborhood of cell (ij)}}$$

if ($s_{kl}^t > s_{avg}$) then $E := E \cup (k,l)$;

until *{further elimination is impossible}*;

for each $(k,l) \in X(i,j)-E$ do

$$f_{kl} := f_{kl} + (s_{avg} - s_{kl}^t)$$

end;

procedure update_water ();

for each *cell* (i,j) do

$$w_{ij}^{t+1} = w_{ij}^t + f_{ij};$$

Algorithm 2 The CA model of anastomosing river

repeat

supply_water (); *{add water to the inlets}*

remove_water (); *{remove water from the outlets}*

calculate_flow (); *{calculate amount of water distributed between the cells}*

update_water (); *{update water in cells}*

distribute_nutrients (); *{calculate nutrients distribution}*

update_peatbog (); *{update peat bog thickness}*

update_terrain (); *{update the height of the terrain}*

until *the_number_of_timestep* $> T$

procedure distribute_nutrients ();

for each *cell* (i,j) do begin

if $w_{ij}^t > 0$ than $n_{ij}^{t+1} = 1$;

if $n_{ij}^t < \max(\{n_{kl}\})$ than $n_{ij}^{t+1} = \gamma \cdot \max(\{n_{kl}\})$ and $(k,l) \in X(i,j)$;

end;

procedure update_peatbog ();

for each *cell* (i,j) do begin

$$\text{if } w_{ij}^t = 0 \text{ than } p_{ij}^{t+1} = p_{ij}^t + \rho n_{ij}^t;$$

end;

procedure `update_terrain ()`;

for each *cell* (*i,j*) do begin

 if $w_{ij}^t > 0$ then $g_{ij}^{t+1} = g_{ij}^t + w_{ij}^t$;

end;

2. Coarse-grained cellular automata model – procedures and algorithms

Algorithm 3 The coarse-grained model of anastomosing river

repeat

update_throughput ();

update_flows ();

 for each (*i,j*) $\in V_G$ do begin

 if $\exists f_{ij} > r_{ij}$ then {flow is jammed}

new_stream (); {create new channel}

 endfor

distribute_nutrients (); {calculate nutrients distribution}

update_peatbog (); {update peat bog thickness}

update_terrain (); {update the height of the terrain}

until *the_number_of_timestep* $> T$

procedure `new_stream` ();

repeat

$H_{kl} = \text{min_height}(H_{ij}; X(v_{ij}))$; {where $H_{ij} = g_{ij} + p_{ij}$ }

 if $H_{kl} < H_{ij}$ then begin

$V_G = V_G \cup \{v_{kl}\}$;

$E_G = E_G \cup \{(v_{kl}, v_{ij})\}$;

$v_{ij} = v_{kl}$;

 end else **find_way_from_cupping** ();

until $(v_{kl} \in V_G) \vee \{\text{mesh border}\}$;
